# The effect of 2,2,2-trifluoroethanol on water studied by using third derivatives of Gibbs energy, G

Ohgi, Hiroyo; Imamura, Hiroshi; Yonenaga, Kazuki; Morita, Takeshi; Nishikawa, Keiko ; Westh, Peter; Koga, Yoshikata

*Published in:*
Journal of Molecular Liquids

*DOI:*
10.1016/j.molliq.2016.09.101

*Publication date:*
2016

*Document Version*
Peer reviewed version

*Citation for published version (APA):*
Ohgi, H., Imamura, H., Yonenaga, K., Morita, T., Nishikawa, K., Westh, P., & Koga, Y. (2016). The effect of 2,2,2-trifluoroethanol on water studied by using third derivatives of Gibbs energy, G. *Journal of Molecular Liquids*, *224A*, 401-407. https://doi.org/10.1016/j.molliq.2016.09.101

# The Effect of 2,2,2-Trifluoroethanol on Water Studied by Using Third Derivatives of Gibbs Energy, *G*

Hiroyo Ohgi,[a] Hiroshi Imamura,[a,b] Kazuki Yonenaga,[a] Takeshi Morita,[a] Keiko Nishikawa,[a] Peter Westh,[c] and Yoshikata Koga. [d] *

[a] Graduate School of Advanced Integration Science, Chiba University, Chiba 263-8522, Japan

[b] The present address: Biomedical Research Institute, National Institute of Advanced Industrial Science and Technology, 1-1-1, Higashi, Tsukuba, Ibaraki 305-8566, Japan

[c] NSM Research Unit for Functional Biomaterials, Roskilde University, Roskilde DK-4000, Denmark

[d] Department of Chemistry, The University of British Columbia, Vancouver, BC. Canada V6T, 1Z1

Abstract

We determined the excess partial molar enthalpy and the excess partial molar volume, $H_{TFE}^{E}$, $V_{TFE}^{E}$, of 2,2,2-trifluoroethanol (TFE) in TFE-$H_2O$ at 25.0 ˚C. We then evaluate the TFE-TFE interactions in terms of enthalpy and volume, $H_{TFE\text{-}TFE}^{E}$ and $V_{TFE\text{-}TFE}^{E}$, graphically without resorting to any model dependent fitting functions. Both model-free third derivatives indicate that TFE is a hydrophobic solute and that as other hydrophobic alkyl mono-ols there are three distinct mixing schemes, Mixing Scheme I, II, and III in their aqueous solutions. The relative strength in hydrophobicity between TFE and *tert*-butylalcohol (TBA), for example, gave a mixed message within the behavior of these third derivative quantities. We thus applied the 1-propanol(1P) probing methodology (Koga, Y. *Phys. Chem. Chem. Phys.* **2013**, *15*, 14548) and quantified the degree of hydrophobicity of TFE. It turned out that TFE is a stronger hydrophobe than 1P and ethanol (ET), and has approximately the same hydrophobicity as TBA within the estimated uncertainty. These findings were compared with the ability reported in literature to denature β-lactoglobulin and to induce α-helices in melittin in their aqueous solutions.

## Introduction

The wordings, hydrophilicity, amphiphilicity and hydrophobicity are loosely defined based on human experiences. Even at the present time, what dissolves readily in water is often called “hydrophilic” and what does not “hydrophobic”. “Amphiphiles” are understood to combine moieties that are typically seen in respectively soluble- an insoluble compounds and sometimes form micelles. A step towards more scientific definition is to take the sign and the value of the hydration free energy of a given solute as a one-dimensional scale for hydrophilicity/amphiphilicity/hydrophobicity.[1, 2] In an attempt to provide a more detailed quantification of hydrophobicity and hydrophilicity, we have developed a differential approach in solution thermodynamics and applied it to study aqueous solutions. We believe that the higher the order of derivative of $G$, the resulting thermodynamic quantity contains more detailed information. Thus, we have experimentally determined the second derivative quantities, excess partial molar enthalpy, $H_i^E$, entropy, $S_i^E$, and volume, $V_i^E$, of solute i, and response functions, $C_p$, $\kappa_T$ and $\alpha_p$. We then raise one more derivative with respect to molar amount of solute i and obtain for example the enthalpic interaction, $H_{i-i}^E$ (defined below), numerically or graphically without resorting to any model dependent fitting function. We learned from the behavior of these model-free third derivative quantities a variety of new

insights into the molecular level scenario of mixing or mixing schemes in aqueous solutions.[3, 4] We learned first that aqueous solutions are in general consisting of three distinctive mole fraction regions in each of which the mixing scheme is qualitatively different from the other two. In the most $H_2O$-rich region, what we call Mixing Scheme I is operative whereby the integrity as liquid $H_2O$ is retained. By that we mean liquid $H_2O$ is an assembly of $H_2O$ molecules via highly fluctuating hydrogen bonds and yet the hydrogen bond network is bond-percolated under ambient conditions. Within Mixing Scheme I the solute modifies the molecular organization of $H_2O$ somewhat crucially depending on the nature of solute; its hydrophobicity/amphiphilicity/hydrophilicity, but the hydrogen bond percolation is not yet broken. In the intermediate mole fraction region, two kinds of clusters mix physically; one rich in $H_2O$ and the other in solute molecules. One may say the solute molecules start to aggregates together in this region. We call this Mixing Scheme II. In the most solute-rich region, where Mixing Scheme III is operative, solute molecules cluster together as in its pure liquid state to which $H_2O$ molecules interact almost as a single gas-like molecule.

We learned these mixing schemes from the behavior of the i-i enthalpic interaction, $H_{i-i}^{E}$, defined as,

$$H_{i\text{-}i}{}^{\mathrm{E}} \equiv N\,(\partial H_i^{\mathrm{E}} / \partial n_i) = (1\text{-}x_i)\,(\partial H_i^{\mathrm{E}} / \partial x_i), \qquad (1)$$

where superscript E stands for excess quantity, $N = \sum n_i$ is the total molar amount, $x_i$ represents the mole fraction of $i$-th component, and the excess partial molar enthalpy of solute i, $H_i^E$ is defined as,

$$H_i^{\mathrm{E}} \equiv (\partial H^{\mathrm{E}} / \partial n_i). \qquad (2)$$

Since $H^{\mathrm{E}}$ is obtained from the first derivative of $G$ with $T$, $H_i^{\mathrm{E}}$ is the second and $H_{i\text{-}i}^{\mathrm{E}}$ the third derivatives respectively. Analogously, the third derivative quantities for entropy, and volume are expressed by changing $H$ to $S$ and $V$ respectively. The mole fraction dependence pattern of $H_{i-i}^E$ for various kinds of solute can be summarized schematically as shown in Fig. 1. Although mono-ols do contain a hydrophilic moiety, -OH, together with a hydrophobic alkyl group, all mono-ols except for methanol show the hall mark of hydrophobic solutes as shown in Fig. 1. Namely, they show a peak type anomalies in $H_{i-i}^E$ pattern and its peak top grows higher and its $x_i$-locus of the peak becomes smaller as the size of alkyl group increases. Similar trends have been observed recently for alkyl-amines.[5, 6] We realized that just as for alkyl carboxylate anions,[7] the hydrophilic end is hydrated with probably a single $H_2O$ molecules and leaves the bulk $H_2O$ away from the hydrated hydrophilic end unperturbed, which leaves the hydrophobic end to interact with $H_2O$ hydrophobically. Typical hydrophiles such as urea and glycerol show the $H_{i-i}^E$ pattern (d),

a complete opposite of hydrophobes in the most $H_2O$-rich region bounded at point X in the figure. Amphiphiles show type (b) or type (c), in between types (a) and (d). We note that the values and their $x_i$-dependences are similar in Mixing Scheme II and III regardless of the nature of solute. Thus, we propose to use the findings sketched in Fig. 1 to redefine hydrophilicity/amphiphilicity/hydrophobicity of a given solute i within Mixing Scheme I.[3, 8]

The manner by which the solute modifies the molecular organization of $H_2O$ within Mixing Scheme I depends crucially on the nature of solute, as mentioned above. Hydrophobes form hydration shells, the hydrogen bond probability of which is enhanced somewhat, but more importantly the hydrogen bond probability of bulk $H_2O$ away from the hydration shells is reduced progressively. . As the solute mole fraction increases to the threshold value depending on the strength of the solute's hydrophobicity, the hydrogen bond network is no longer bond-percolated and the system goes into the crossover region from point X to Y. Mixing Scheme II then becomes operative beyond point Y.

Hydrophiles, on the other hand, form hydrogen bonds directly to the existing hydrogen bond network of $H_2O$ and pin down the inherent $S$-$V$ cross fluctuation of pure $H_2O$ by breaking the H donor-acceptor symmetry of pure $H_2O$. When the solute mole fraction reaches about 0.1, there is no more bulk $H_2O$ available to speak of percolated hydrogen bond

network and the system crossover to Mixing II more gradually than for hydrophobes. Amphiphiles' hydrophobic and hydrophilic moieties seem to work additively on the molecular organization of $H_2O$. These findings are from accumulation of a large number of experimental observations of the behavior of the second and the third derivative qunatities.[3, 4, 8-12]

Here we use the same methodology to study aqueous solutions of 2,2,2-trifluoroethanol (TFE). TFE has been receiving much attention for its marked ability to change structures of various proteins and peptides in aqueous solutions.[13-21] Its effect is greater than estimated from relative dielectric constants of respective alcohols. For example, although TFE and ethanol (ET) have almost the same dielectric constants, structural changes of proteins and peptides in aqueous solutions need a lesser concentration of TFE than ethanol; the amount needed for TFE is less than a half of that of ethanol in the mole fraction of alcohol.[20, 21] Molecular mechanisms responsible for this have been debated for about five decades,[15] and yet the debate is far from reaching a consensus. For TFE-$H_2O$, there have been a number of thermodynamic,[22, 23] scattering and NMR,[24, 25] and MD simulation studies.[26, 27] To our knowledge, none except ref. 24 recognized the three distinct mole fraction dependent mixing schemes. Takamuku et al. using scattering techniques concluded

that in the range of the mole fraction of TFE, $x_{TFE} < 0.1$ the tetrahedral-like structure of $H_2O$ is enhanced, at $x_{TFE} \approx 0.15$ TFE clusters form and at $x_{TFE} \approx 0.7$ there is a break in the number of O···O hydrogen bonds.[24] Though not explicitly stated, in effect there are three distinct mixing schemes in TFE – $H_2O$, including the I - II crossover region from point X to Y and that TFE is a hydrophobe. Their boundary values are listed in Table 1. Here we reexamine TFE – $H_2O$ by our differential approach in solution thermodynamics. In particular, we first experimentally determine the excess partial molar enthalpy of TFE, $H_{TFE}^{E}$, and take derivative with respect to $x_{TFE}$ graphically without resorting to any fitting functions to obtain the model-free TFE-TFE enthalpic interaction by,

$$H_{TFE\text{-}TFE}^{E} \equiv N\,(\partial H_{TFE}^{E} / \partial n_{TFE}) = (1\text{-}x_{TFE})\,(\partial H_{TFE}^{E} / \partial x_{TFE}). \qquad (3)$$

To calculate the volumetric third derivative, $V_{TFE\text{-}TFE}^{E}$, we determine the density, $\rho$ of TFE-$H_2O$ binary mixture very accurately and then the excess molar volumes are calculated by,

$$V_m^{E} = \{(x_{TFE}\,M_{TFE}^{*} + x_w\,M_w^{*}) / \rho\} - \{x_{TFE}\,V_{TFE}^{*} + x_w\,V_w^{*}\}, \qquad (4)$$

where $M_{TFE}^{*}$ and $M_w^{*}$ are the molecular weights of TFE and $H_2O$ respectively, and $V_{TFE}^{*}$ and $V_w^{*}$ are the molar volumes of pure components. We obtain the excess partial molar volumes of TFE and $H_2O$, $V_{TFE}^{E}$ and $V_w^{E}$, from $V_m^{E}$ as,

$$V_{TFE}^{E} = (1\text{-}x_{TFE})\,(\partial V_m^{E} / \partial x_{TFE}) + V_m^{E}, \qquad (5)$$

$$V_w^E = (1\text{-}x_w)\,(\partial V_m^E / \partial x_w) + V_m^E. \quad (6)$$

$V_{TFE\text{-}TFE}^E$ is then calculated according to,

$$V_{TFE\text{-}TFE}^E \equiv N\,(\partial V_{TFE}^E / \partial n_{TFE}) = (1\text{-}x_{TFE})\,(\partial V_{TFE}^E / \partial x_{TFE}). \quad (7)$$

Furthermore, we evaluate the degree of TFE's hydrophobicity by the 1-propanol (1P) probing methodology, detailed elsewhere.[12] Briefly, we first dissolve the chosen test sample (S) within its Mixing Scheme I with the initial mole fraction of test sample S, $x_s^0 = n_s / (n_s + n_w)$ and let S modifies $H_2O$. We then evaluate the nature and the degree of its modification by the induced changes in the pattern of $H_{1P-1P}^E$ by the presence of S. After experimentally determining $H_{1P}^E$, we calculate the 1P-1P enthalpic interaction, $H_{1P\text{-}1P}^E$, in the ternary 1P-S-$H_2O$ system in a similar manner as in eq. (3) as,

$$H_{1P\text{-}1P}^E \equiv N\,(\partial H_{1P}^E / \partial n_{1P}) = (1\text{-}x_{1P})\,(\partial H_{1P}^E / \partial x_{1P}). \quad (8)$$

As discussed elsewhere,[12] the $x_{1P}$–dependence pattern of $H_{1P\text{-}1P}^E$ shifts in the direction and the degree depending on the nature of S. Namely the peak top of $H_{1P\text{-}1P}^E$ shifts to the west (to a smaller value of $x_{1P}$) when test sample S is hydrophobic and to the south if S is hydrophilic. The former westward shift is related to forming hydration shells, and the latter shift is related to how strongly the solute affects the *S*-*V* cross fluctuation of the system. The shifts of the peak top are linear to $x_s^0$. We thus call the slope of westward shift of point X against $x_s^0$ as

the index of hydrophobicity, *a*. That of northward/southward is the index of hydrophilicity, *b* (the northward shift is regarded as negative hydrophilicity). Using these two indices, hydrophobicity and hydrophilicity of the test sample S are displayed on a two-dimensional map. We point out that this 1P-probong methodology seeks the variation of $H^{E}_{1P-1P}$, the third derivative quantity, on addition of the test sample S. In effect, therefore, this methodology uses the fourth derivative of *G*.

## Experimental

### *Titration calorimetry*

2,2,2-trifluoroethanol (TFE) (Sigma-Aldrich, >99.0%) and 1-propanol (1P) (Sigma-Aldrich, >99.9%) were used as supplied. Deionized $H_2O$ was prepared using Milli-Q (EMD Millipore, Bilerica, MA). The excess partial molar enthalpies of TFE and 1P , $H_{\mathrm{TFE}}{}^{\mathrm{E}}$ and $H_{1\mathrm{P}}{}^{\mathrm{E}}$, were determined by TAM III semi-isothermal titration calorimeter (TA Instrument, New Castle, DE) at 25.0000±0.0001 ˚C (nominal) in the dynamic correction mode.[28-30] A 700 μL sample of water or TFE solution was quantified by weight in a 1 mL stainless steel cell and mounted on the calorimeter. The solution was subsequently titrated with 7.94 μL aliquots of TFE, or with 6.46 μL aliquots of 1P. For the case that the initial concentration of TFE was 0,

$x_{TFE}^0$ = 0, the injection volume of 1P was 3.92 μL. The injecting duration was 10 s. The thermal effect of each injection was converted to the quotient $\delta H^E / \delta n_i$, where $\delta n_i$ is the titrant amount of $i$ = TFE or 1P. The ratio of the titrant over the titrand was in the order of $10^{-2}$, and the quotient could be approximated as the partial derivative of eq. (2).[31] The interval of injection was 15 min for the measurements of $H_{TFE}^E$. For $H_{1P}^E$, 15 min interval was used when $x_{TFE}^0$ = 0. It was increased to 20 min otherwise. The uncertainty is estimated as ±0.05 kJmol$^{-1}$.

For the series of the 1P-probing study of the effect of TFE on $H_2O$ at $x_{TFE}^0$ = 0.02499, a homemade titration calorimeter was used of a similar design to the LKB Bromma titration calorimeter, as described elsewhere,[32] except that a stepping-motor-driven syringe system (Chemyx, Fusion 100) with a 25 mL Hamilton syringe was used to deliver the titrant 1P. $H_2O$ was purified by Milli-Q system. TFE (Fluorochem, 99 %) and 1P (Sigma-Aldrich, >99.9%) were used as supplied. For this series the uncertainty is somewhat larger than that by TAM system. As will become evident below in Fig. 6, the data seem acceptable for direct comparison with the series using TAM III.

*Density measurement*

TFE, (Fluorochem, 99%) was used as supplied. Solutions were prepared gravimetrically using deionized $H_2O$, prepared using Milli-Q system. Densities of the TFE solutions were determined with DMA4500 density/specific gravity/concentration meter (Anton Paar, Graz, Austria), which has an oscillating U-tube. Calibration with air and water was performed every day before the measurement. The temperature was kept at 25.00±0.03 ˚C. The uncertainty of density is ±0.00005 $gcm^{-3}$.

Results and discussion

*Enthalpic interaction of TFE molecules in TFE-$H_2O$ binary mixture*

The values of the excess partial molar enthalpy of TFE, $H_{TFE}^{E}$ are listed in Table S1 (Supplementary data) and plotted in Fig.2 (a). As our aim is to obtain higher order derivative quantities, we take derivative of $H_{TFE}^{E}$ graphically with respect to $x_{TFE}$ and obtain the enthalpic TFE-TFE interaction, $H_{TFE\text{-}TFE}^{E}$ by eq. (3). The results are shown in Fig.2 (b). The interval for graphical differentiation was taken as $\delta x_{TFE} = 0.008$.[31] The uncertainty is estimated as ±5 $kJmol^{-1}$. It is clear that $H_{TFE\text{-}TFE}^{E}$ shows a peak type anomaly, suggesting TFE is a hydrophobic solute as alkyl mono-ols. The results for point X and Y are listed in Table 1, together with those for alkyl alcohols.[33] In the table, it is evident that as the size of

alkyl group increases, the $x_{AL}$ (mole fraction of alkyl mono-ols) locus of point X decreases, and its value of $H^{E}_{AL-AL}$ becomes larger. If this trend is applicable for TFE, TFE should be a stronger hydrophobe than ET as well as 1P, from the point of view of the mole fraction locus of point X. From the peak height point of view, on the other hand, TFE is a weaker hydrophobe than 1P but stronger than ET. Before settling this issue, we evaluate volumetric third derivatives.

*Volumetric interaction of TFE molecules in TFE-$H_2O$ binary mixture*

We calculated the excess partial molar volume of TFE, $V_{TFE}^{E}$ using the density data, which are listed in Table S2 (Supplementary data). The resulting values of $V_{TFE}^{E}$ are shown in Fig.3 (a). The uncertainty is estimated as ± 0.07 $cm^3mol^{-1}$. As discussed extensively elsewhere,[9-11] the initial decrease of $V_{TFE}^{E}$ is consistent with the detailed mixing scenario of Mixing Scheme I for hydrophobic solutes.

In the TFE-rich region, i.e. $x_{TFE} > 0.72$, $V_{TFE}^{E}$ is almost zero and constant, the boundary of which is shown by the arrow in Fig.3 (a). This means that in this TFE-rich region, TFE molecules breaking away from its pure state settle in TFE-$H_2O$ solution, and see no difference in terms of its volumetric situation. Thus, we suggest that TFE

molecules form clusters of their own kind, as in its pure state.[8] This corresponds to Mixing Scheme III and the Mixing Scheme II-III boundary is at about $x_{TFE} \sim 0.72$. This boundary is rather hard to pin point as is evident from Fig.3 (a). We thus calculate the excess partial molar volume of $H_2O$, $V_w^E$, taking an advantage that the II-III boundary is more conspicuous in $V_w^E$. As shown in Fig.3 (b), we now identify the II-III boundary to be at $x_{TFE} \sim 0.73$ with more confidence.

Next, we evaluate the volumetric TFE-TFE interaction, $V_{TFE\text{-}TFE}^E$, by taking derivative of $V_{TFE}^E$ graphically again. The results are shown in Fig. 4. The interval for graphical differentiation was taken as $\delta x_{TFE} = 0.008$[31] for $0 < x_{TFE} < 0.40$ and $\delta x_{TFE} = 0.04$ for $0.40 < x_{TFE} < 1$. The peak type anomaly evident in the figure, is typical for hydrophobic solutes.[8] The point X appears at $x_{TFE} = 0.04$ with $V_{TFE\text{-}TFE}^E = 94$ cm$^3$ mol$^{-1}$. The locus of $x_{TFE}$ at point X is the same as that from $H_{TFE\text{-}TFE}^E$, Fig.2 (b), as it should be, although that of point Y is about 0.1, a little larger than that determined by $H_{TFE\text{-}TFE}^E$, Fig. 2(b). Considering the fact that $V_{TFE\text{-}TFE}^E$, Fig. 4, is the results of double graphical differentiation of the experimental density data, we take the value of 0.07 from the behavior of $H_{TFE\text{-}TFE}^E$, Fig. 2(b), which is the result of a single differentiation of the experimental data, $H_{TFE}^E$. Since the information given by the behavior of point X of the $H_{i-i}^E$ pattern is

rather mixed, in the next section we make an attempt at quantifying the difference in hydrophobicity between alkyl mono-ols and TFE, by using the 1P-probing methodology, which in effect utilizes the fourth derivative quantity.

*1-propanol probing methodology for TFE*

We apply the 1-propanol (1P) probing methodology detailed elsewhere[12] in order to quantify the degree of hydrophobicity of TFE in two dimensional scale for comparison with those of alkyl mono-ols. The methodology utilize the variation of the $x_{1P}$-dependence pattern of $H_{1P\text{-}1P}{}^{E}$, a third derivative quantity, on addition of TFE in the ternary system 1P-TFE-$H_2O$. Thus, it can be regarded in effect as using the fourth derivative, as mentioned above. Hence a more quantitative distinction could be expected.[12] Briefly we deal with a three-component system, 1P-S-$H_2O$, where S is the test sample the degree of hydrophobicity/hydrophilicity of which is to be determined. In the present case, S is TFE.

Fig.5 is a schematic description of $H_{1P\text{-}1P}{}^{E}$ patterns against $x_{1P}$ and their induced changes on addition of hydrophobic test samples, S.[12] In this figure, the broken line (marked [0]) represents $H_{1P\text{-}1P}{}^{E}$ for binary 1P-$H_2O$. The case [A] represents the effect of almost equally hydrophobic 2-propanol (2P) as 1P. Consider the case where 1P itself is

treated as S, then 1P added as S brings the system a part way to the north-east along the dotted line [0] in the figure and the probing 1P then takes the system the remaining way to point X. This results in case [A], a parallel shift to the west, to a smaller value of $x_{1P}$. The case [B] is found with a weaker hydrophobe than 1P such as ethanol (ET). The case [C] occurs with a stronger hydrophobic S than 1P such as *tert*-butylalcohol (TBA). These north-south shifts of point X are related to the effect of hydrophobic S on the hydrogen bond probability of bulk $H_2O$ away from hydration shells.[12]

The results of excess partial molar enthalpies of 1P, $H_{1P}^{E}$, in the mixed solvent TFE-$H_2O$ are listed in Table S3 (Supplementary data) and plotted in Fig.6. As indicated in the figure, the data were taken by two sets of equipment. This was described in the experimental section. As is evident in Fig. 6, the results for the binary case, i.e. $x_{TFE}^{0} = 0$, by the both systems can be regarded consistent with each other, and a single smooth curve can be drawn. Thus, the data for the case of $x_{TFE} = 0.02499$ by the home-made system could be equally utilized together with those by TAM III. Given the data of $H_{1P}^{E}$ we drew smooth curves through all the data points of Fig. 6 using a flexible ruler and read the data off the smooth curves drawn at the interval of $\delta x_{1P} = 0.004$.[31] We did this in duplicate independently, and calculated the enthalpic 1P-1P interaction, $H_{1P\text{-}1P}^{E}$ with the intervals of

$\delta x_{1P} = 0.008$. The result is shown in Fig.7. Only the results from a single data analysis are displayed in the figure for clarity of display. The uncertainty for $H_{1P\text{-}1P}^{E}$ is estimated from the discrepancy between both sets of results as ± 6 kJmol$^{-1}$. As the figure indicates, the peak tops, point X, shifts westward progressively and northward slightly on increasing the initial mole fraction of TFE, $x_{TFE}^{0}$. The westward and northward shifts of point X against $x_{TFE}^{0}$ are plotted in Fig. 8 (a) and (b). The slope of the $x_{1P}$ loci against $x_{TFE}$ in Fig.8(a) corresponds to the hydrophobicity index, $a$, and that in Fig.8(b) is the hydrophilicity index, $b$.[12] We determined the indices as $a = -1.07 \pm 0.05$ and $b = 910 \pm 300$ kJmol$^{-1}$.

These values of $a$ and $b$ are listed in Table 2 together with those for alkyl mono-ols determined earlier,[12, 34-40] and plotted in Fig 9. The origin of the map corresponds to $H_2O$, and the probing 1P should be at (-1, 0). Relative to these two points, stronger hydrophobes than the probing 1P spread to the north-west direction. In addition, weaker hydrophobes are placed in the south-west quadrant. If ethanol (ET) was to be used as the probe, for example, then ethanol must be plotted at (-1, 0) and the remaining mono-ols must spread towards the north-west. About methanol (ME), however, we found recently that it should be classified as amphiphile.[40] As is evident from Table 2 and Fig. 9, TFE turns out to be a stronger hydrophobe than ET, 2P and 1P, but has almost the same hydrophobicity as for TBA.

It is also obvious from the figure that TFE is more hydrophobic than ethanol even though the number of carbon atoms is the same. Fluorine atoms attached to C are known to induce hydrophobicity in molecules.[41-43] Indeed, the recent report using the 1P-probing methodology found that trifluoroacetate, $CF_3COO^-$, ions are more hydrophobic than acetate, $CH_3COO^-$ ions.[44]

In order to quantify the relative hydrophobicity on the map, we evaluate the unitless distance of each plot from the origin, *D* defined as,[12]

$$D = \pm \{ ( a / 1.25 )^2 + ( b / 7000 )^2 \}^{1/2}. \qquad (9)$$

The sign is given with a positive sign when the plot is in the north-west quadrant including the abscissa. Those in the south-west quadrant including the negative ordinate are given with a negative sign.[12] It was observed among alkyl mono-ols that the absolute value ranking of *D* is parallel to that of the hydrophobicity.[12] For TFE, the absolute value of $D = 0.87 \pm 0.09$, is larger than ET, 2P, and 1P and almost the same as that for TBA, $0.94 \pm 0.07$. (See the footnote of Table 2). Thus the absolute value of *D* ranks as

$$\text{ME} < \text{ET} < \text{2P} < \text{1P} < \text{TFE} \approx \text{TBA} < \text{BE}. \qquad (10)$$

where BE is the C6 ether, 2-butoxyethanol. This ranking is by the 1P-probing methodology, which is equivalent to using the fourth derivative of *G*. Commonly termed

"hydrophobicity/hydrophilicity" uses hydration free energy or hydration chemical potential. They are zero-th and the first derivative of *G.* Thus, the ranking (10) above by utilizing in effect a fourth derivative could be a finer scale for hydrophobicity. ME being actually an amphiphile,[40] its weakest ranking is only natural.

*Effects of alcohols on proteins and peptides*

As discussed in Introduction, TFE is effective to denature proteins and to induce helices in peptides. Hirota *et al*. [45 - 47] monitored the structural changes on addition of alcohols of β-lactogulobulin and melittin by following the content of α-helix determined by circular dichroism (CD) spectroscopy at 20 ˚C. They argued that denaturation of protein and the conversion of melittin to α-helices share the same fundamental mechanism and that it is the hydrophobic alkyl groups and halogen atoms that are responsible for the processes, while –OH group has a retarding effect. They then defined the effectiveness of each alcohol by the slope of linear fit of the degree of conversion expressed by Δ*G* against the molarity of alcohol. They calculated the degree of conversion, Δ*G*, by assuming the conversion process being described by the two state model. Hence, the resulting slopes for each alcohol represent its effectiveness. In terms of the order of derivative, this corresponds to

the first derivative of *G*. They ranked the "alcohol effects" as,[47]

$$\text{ME}(1.97) < \text{ET}(3.92) < \text{2P}(6.01) < \text{1P}(8.45) < \text{TFE}(9.15) < \text{TBA}(12.0), \qquad (11)$$

for denaturation of β-lactoguloblin, and

$$\text{ME}(0.78) < \text{ET}(1.57) < \text{2P}(3.25) < \text{1P}(3.68) < \text{TBA}(4.75) < \text{TFE}(5.05), \qquad (12)$$

for induction of α-helices of melittin. The numbers in brackets are the slopes of $\Delta G$ against the molarity of alcohol taken from Table 1 of ref. [47]. Thus, their rankings are based on the first derivative of *G*. They claimed that the correlation between the ranking (11) and (12) is good enough to conclude that both processes share the same fundamental mechanism.[47] On the other hand, the D-ranking, eq.(10) based on the fourth derivative of *G*, is equally similar to the both observations (11) and (12). This suggests an importance of the D-ranking based on the fourth derivative of *G,* eq.(10) of aqueous alcohols, on the so called "alcohol effects" on the processes involving biopolymers. Clearly there must be an enormous number of factors which are involved in such processes, working not independently but holistically. We suggest that the details of mole fraction dependent mixing schemes in the aqueous alcohols themselves and the D-ranking by the 1P-probing methodology ought to be taken into account as one such factor.

Acknowledgements

We thank Carlsberg Foundation for donating TAM III isothermal titration calorimeter to PW.

References

1 R. Underwood, J. Tomlinson-Phillips, D. Ben-Amotz, J. Phys. Chem. B 114 (2010) 8646.

2 Y. Zhang, S. Patel, J. Phys. Chem. B 114 (2010) 11076.

3 Y. Koga, Solution Thermodynamics and Its Application to Aqueous Solutions: A Differential Approach, Elsevier, Amsterdam, 2007.

4 S. H. Tanaka, H. I. Yoshihara, A. W.-C. Ho, F. W. Lau, P. Westh, Y. Koga, Can. J. Chem. 74 (1996) 713.

5 K. Zemankova, J. Troncoso, C. A. Cerdeira, L. Romani, Chem. Phys. Lett. 640 (2015) 184.

6 K. Zemankova, J. Troncoso, C. A. Cerdeira, L. Romani, M. A. Anisimov, Chem. Phys. 472 (2016) 36.

7 T. Kondo, Y. Miyazaki, A. Inaba, Y. Koga, J. Phys. Chem. B 116 (2012) 3571.

8 Y. Koga, Netsu Sokutei 30 (2003) 54. Available in a pdf file on request to the author. koga@chem.ubc.ca

9 Y. Koga, J. Phys. Chem. 96 (1992) 10466.

10 Y. Koga, V. J. Loo and K. T. Puhacz, Can. J. Chem. 73 (1995) 1294.

11 Y. Koga, J. Phys. Chem. 100 (1996) 5172.

12 Y. Koga, Phys. Chem. Chem. Phys. 15 (2013) 14548.

13 J. W. Nelson and N. R. Kallenbach, Proteins Struct. Funct. Genet. 1 (1986) 211.

14 A. Jasanoff and A. R. Fersht, Biochem. 33 (1994) 2129.

15 M. Buck,. Q. Rev. Biophys. 31 (1998) 297.

16 D. P. Hong, M. Hoshino, R. Kuboi and Y. Goto, J. Am. Chem. Soc. 121 (1999) 8427.

17 Y. Kumar, S. Muzammil and S. Tayyab, J. Biochem. 138 (2005) 335.

18 N. Rezaei-Ghaleh, M. Amininasab and M. Nemat-Gorgani, Biophys. J. 95 (2008) 4139.

19 T. Imai, A. Kovalenko, F. Hirata and A. Kidera, Interdiscip. Sci. Comput. Life Sci. 1 (2009) 156.

20 K. Matsuo, Y. Sakurada, S. I. Tate, H. Namatame, M. Taniguchi and K. Gekko, Proteins Struct. Funct. Bioinformat. 80 (2012) 281.

21 K. Yoshida, Y. Fukushima and T. Yamaguchi, J. Mol. Liq. 189 (2014) 1.

22 M. J. Blandamer, J. Burgess, A. Cooney, H. J., H. J. Cowles, I. M. Horn, K. J. Martin, K. W. Morcom, J. Chem. Soc. Faraday Trans. 86 (1990) 2209.

23 R. Chitra, P. E. Smith, J. Phys. Chem. B 106 (2002) 1491.

24 T. Takamuku, T. Kumai, K. Yoshida, T. Otomo, T. Yamaguchi, J. Phys. Chem. A 109 (2005) 7667.

25 M. Matsugami, R. Yamamoto, T. Kumai, M. Tanaka, T. Umecky, T. Takamuku, J. Mol. Liq. 217 (2016) 3.

26 R. Chitra, P. E. Smith, J. Chem. Phys. 114 (2001) 426.

27 S. Jalili, M. Akhavan, J. Comput. Chem. 31 (2009) 286.

28 V. E. Calvet and H. Prat, Recent Progress in Microcalorimetry, Pergamon Press, Oxford, 1963.

29 K.-R. Löblich, Thermochim. Acta 231 (1994) 7.

30 B. Löwen, S. Schulz and J. Seippel, Thermochim. Acta 235 (1994) 147.

31 M. T. Parsons, P. Westh, J. V. Davies, C. Trandum, E. C. To, W. M. Chiang, E. G. M. Yee and Y. Koga, J. Solution Chem. 30 (2001) 1007.

32 H. Kato, K. Nishikawa and Y. Koga, J. Phys. Chem. B 112 (2008) 2655.

33 Ref. (3), Table V-3, p.114, and Table V-5, p. 146.

34 Y. Koga, K. Nishikawa and P. Westh, J. Phys. Chem. B 111 (2007) 13943.

35 Y. Koga, J. Solution Chem. 32 (2003) 803.

36 T. Morita, P. Westh, K. Nishikawa and Y. Koga, J. Phys. Chem. B 116 (2012) 7328.

37 J. Hu, W. M. Chiang, P. Westh, D. H. C. Chen, C. A. Haynes and Y. Koga, Bull. Chem. Soc. Jpn. 74 (2001) 809.

38 K. Miki, P. Westh and Y. Koga, J. Phys. Chem. B 109 (2005) 19536.

39 Y. Koga, P. Westh, K. Nishikawa and S. Subramanian, J. Phys. Chem. B 115 (2011) 2995.

40 K. Yoshida, P. Westh, A. Inaba, M. Nakano and Y. Koga, J. Mol. Liq. 202 (2015) 40.

41 M. P. Krafft, Curr. Opin. Colloid Interface Sci. 8 (2003) 213.

42 J. C. Biffinger, H. W. Kim and S. G. DiMagno, ChemBioChem 5 (2004) 622.

43 V. H. Dalvi and P. J. Rossky, Proc. Natl. Acad. Sci. U. S. A. 107 (2010) 13603.

44 T. Morita, K. Miki, A. Nitta, H. Ohgi and P. Westh, Phys. Chem. Chem. Phys. 17 (2015) 22170.

45 N. Hirota, K. Mizuno and Y. Goto, Protein Sci. 6 (1997) 416.

46 N. Hirota, K. Mizuno and Y. Goto, J. Mol. Biol. 275 (1998) 365.

47 N. Hirota-Nakaoka and Y. Goto, Bioorganic Med. Chem. 7 (1999) 67.

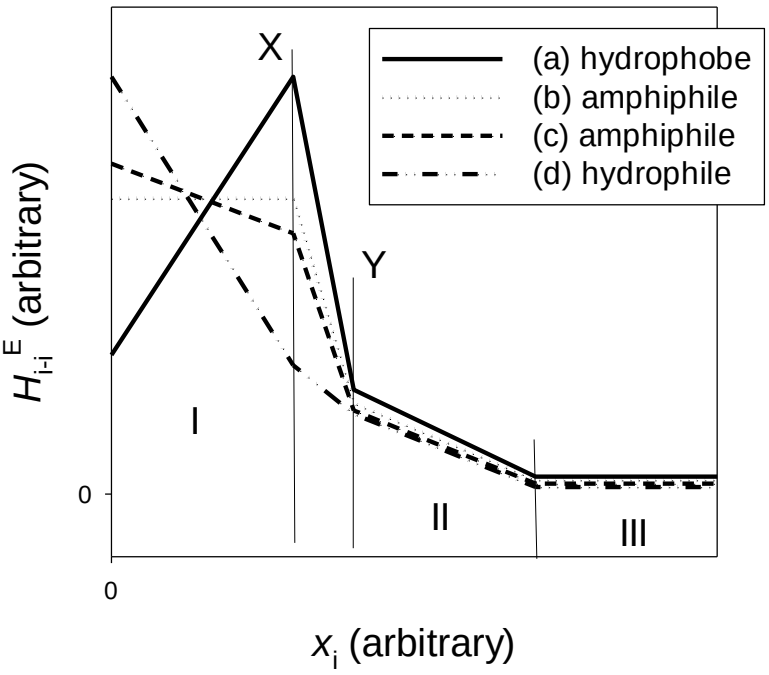


Fig. 1 Schematic sketch of the $x_i$-dependence patterns of $H_{i-i}^{E}$, the enthalpic solute-solute interaction for various solutes i at room temperature. The first break point X is the end of Mixing Scheme I. After crossover region to point Y, Mixing Scheme II starts. We note that the values and the mole fraction dependences in Mixing Schemes II and III are similar independent of the nature of solute i. The boundary between Mixing Scheme II and III is rather blurred. This seems to be a reasonable interpretation of the observations sketched in this figure. See text.

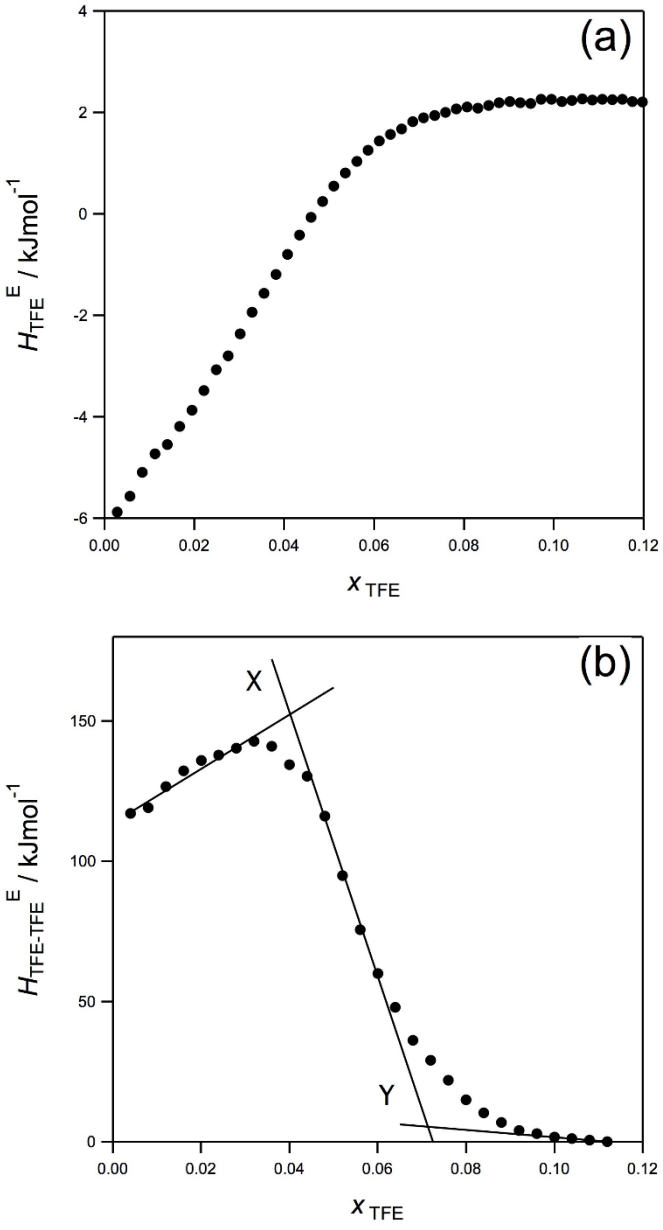


Fig.2 (a) Excess partial molar enthalpy of TFE, $H_{TFE}^{E}$, in TFE-$H_2O$ mixture at 25.0 ˚C. (b) Enthalpic TFE-TFE interaction, $H_{TFE-TFE}^{E}$, in TFE-$H_2O$ mixture at 25.0 ˚C. The fact that the $x_{TFE}$-dependence pattern takes a peak-type anomaly suggests TFE is a hydrophobic solute in aqueous solution.

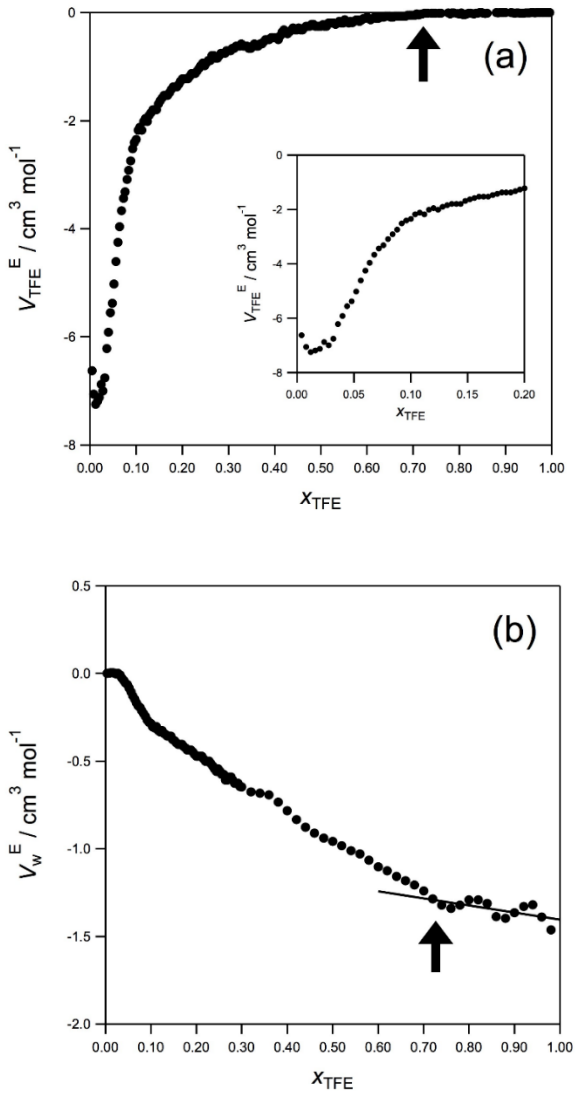


Fig.3 (a) Excess partial molar volume of TFE, $V_{TFE}^{E}$, in TFE-$H_2O$ mixture at 25.0 ˚C. The inset shows the graph in which the $H_2O$ rich region is expanded. $V_{TEF}^{E}$ shows a clear initial decrease in the inset, which is the same behavior as other alkyl mono-ols, typical hydrophobes. (b) Excess partial molar volume of $H_2O$, $V_{w}^{E}$, in TFE-$H_2O$ mixture at 25.0 ˚C. From the locus of the arrow the boundary from Mixing Scheme II to III was determined as $x_{TFE} = 0.73$. See text.

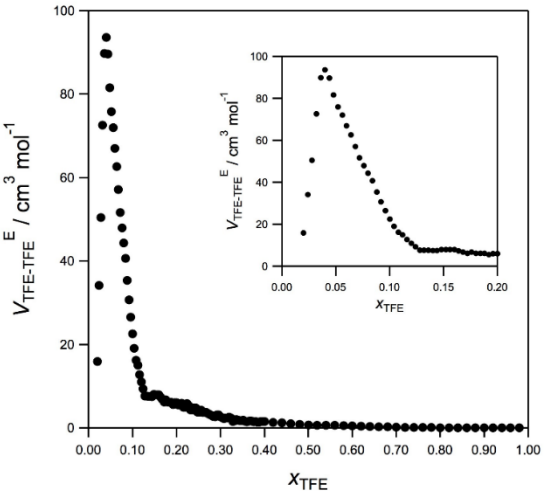


Fig.4 Volumetric TFE-TFE interaction, $V_{TFE\text{-}TFE}^{E}$, in TFE-$H_2O$ mixture at 25.0 ˚C. The inset shows the graph in which the $H_2O$ rich region is expanded. A peak type anomaly is evident suggesting that TFE is a hydrophobe.

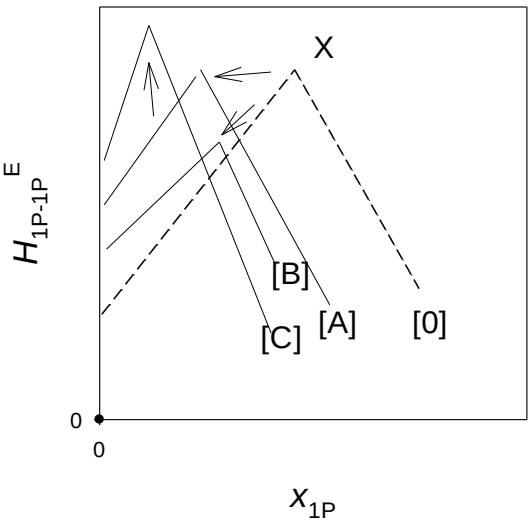


Fig.5 The $H_{1P\text{-}1P}^{E}$ pattern changes by the presence of hydrophobic samples (S) in 1P-S-$H_2O$ mixture. [0]; binary 1P-$H_2O$. [A]; the mixture with an equally hydrophobic S as 1P. [B]; the mixture with a weaker hydrophobic S than 1P. [C]; the mixture with a stronger hydrophobic S than 1P.

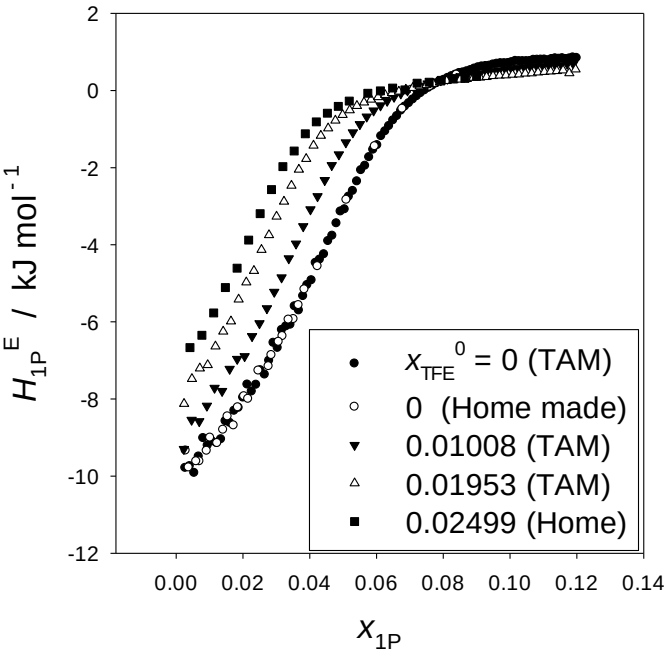


Fig.6 Excess partial molar enthalpy of 1P in 1P-TFE-$H_2O$ mixture at 25.0 ˚C. For all the series, sigmoidal increases are evident with inflection points. The series designated as (TAM) were obtained using a TAM III calorimeter, while those as (Home) were the results by using the home-made calorimeter. See text for detail.

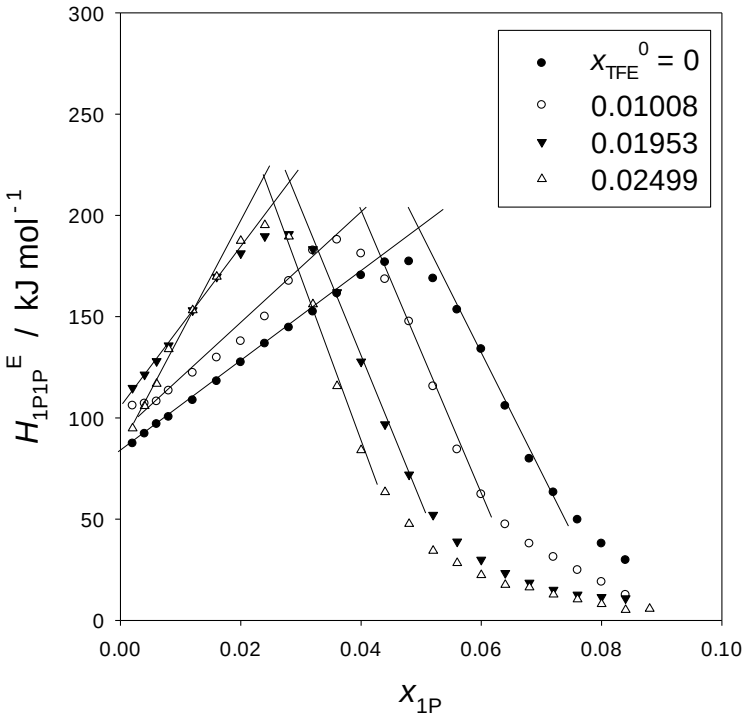


Fig.7 Enthalpic 1P-1P interaction, $H_{1P\text{-}1P}^{E}$, in 1P-TFE-$H_2O$ mixture at 25.0 ˚C and its induced shifts by the presence of TFE. Peak tops shift to the west (to a smaller value of $x_{1P}$) and slightly to the north (to a larger value of $H_{1P\text{-}1P}^{E}$) as $x_{TFE}$ increases. This indicates TFE is a stronger hydrophobe than probing 1P.

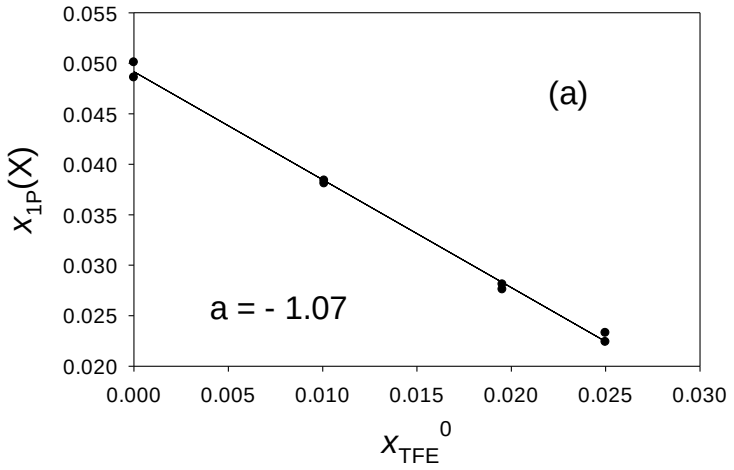


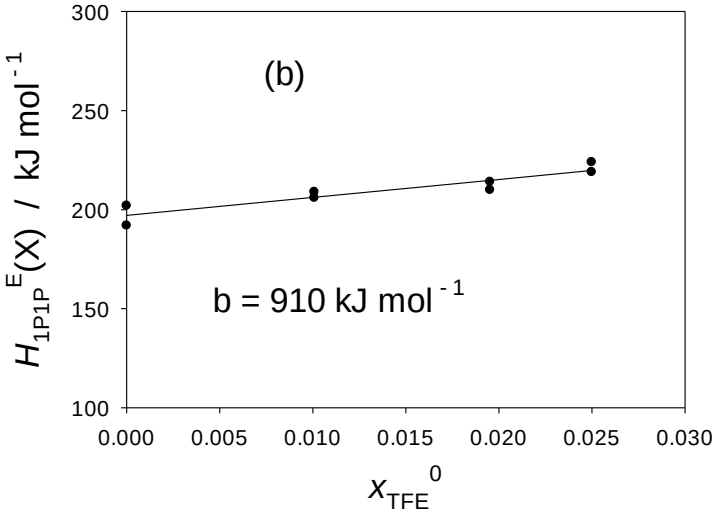


Fig.8 (a) The $x_{1P}$ loci of point X against the initial mole fraction of TFE, $x_{TFE}^{0}$. The plots are linear and its slope is defined as the hydrophobicity index, *a.* (b) The $H_{1P\text{-}1P}^{E}$ loci of point X against the initial mole fraction of TFE, $x_{TFE}^{0}$. The plots seem to be linear, the slope of which provides the hydrophilicity index, $b$/kJ· mol$^{-1}$.

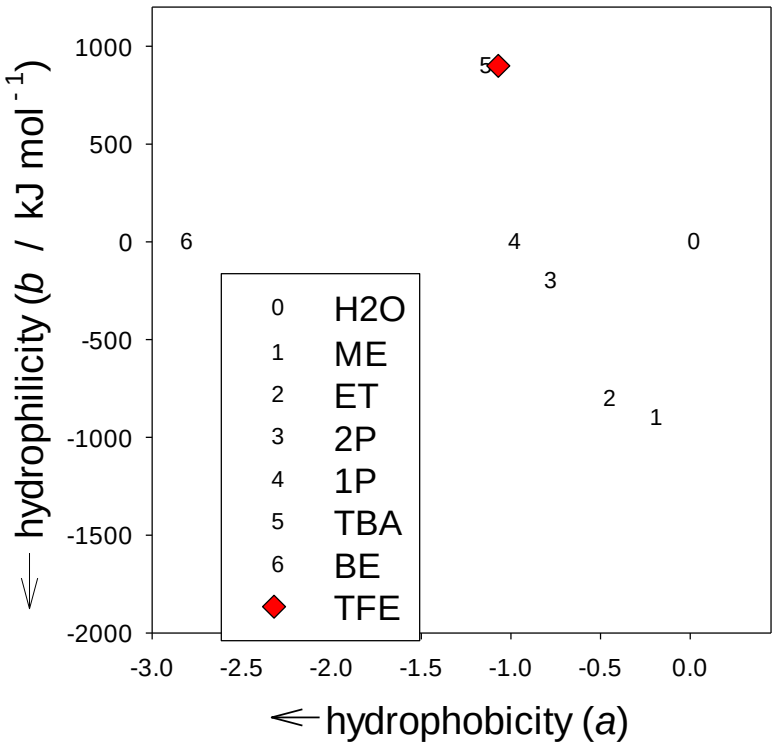


Fig.9 The hydrophobicity/hydrophilicity map for alcohols. The coordinates (*a, b*) for TFE are determined in this work. The remaining ones are taken from our previous works as referenced in Table.2. The distance from the origin is defined as the strength of hydrophobicity among alkyl mono-ols larger than ET. Its ranking runs as ET<2P<1P<TBA<BE, consistent with the size of alkyl group. It is therefore striking that TFE has about the same strength as TBA. See text.

Table 1. Summary of the behaviors of $H_{AL\text{-}AL}^{E}$ for AL = TFE and other alkyl mono-ols at 25 ºC.

| AL* | $x_{AL}$ at point X | $H_{AL\text{-}AL}^{E}$ at X kJ· mol$^{-1}$ | $x_{AL}$ at Y | $H_{AL\text{-}AL}^{E}$ at Y kJ· mol$^{-1}$ | $x_{AL}$ at II-III | Ref. |
|---|---|---|---|---|---|---|
| TFE | 0.040 | 150 | 0.072 | 5 | 0.73 | This |
| TFE | <0.1 | | ~0.15 | | ~0.7 | [24] |
| ME | 0.07 | 32 | 0.25 | | 0.57 | [33] |
| ET | 0.06 | 73 | 0.19 | | 0.76 | [33] |
| 2P | 0.05 | 180 | 0.11 | | 0.88 | [33] |
| 1P | 0.049 | 210 | 0.09 | | 0.80 | [33] |
| TBA | 0.045 | 350 | 0.065 | | none | [33] |
| BE | 0.017 | 1100 | 0.021 | | 0.65 | [33] |

*The abbreviations for alcohols (AL) are 2,2,2-trifluoroethanol (TFE), methanol (ME), ethanol (ET), 2-propanol (2P), 1-propanol (1P), tert-butanol (TBA) and 2-butoxyethanol (BE).

Table.2 The coordinates of each sample in the hydrophobicity/hydrophilicity map by the 1P-probing methodology and distance from the origin, D.

| Symbols in Fig. 8 | Samples | a | b / kJmol$^{-1}$ | D | Ref. |
|---|---|---|---|---|---|
| 0 | $H_2O$ | 0 | 0 | 0.00 | [34] |
| 1 | ME | -0.21 | -905 | -0.21 | [35] |
| 2 | ET | -0.47 | -788 | -0.39 | [36] |
| 3 | 2P | -0.80 | -167 | -0.64 | [37] |
| 4 | 1P | -1.00 | 0 | 0.80 | [34] |
| 5 | TBA* | -1.16 | 890 | 0.94 | This* |
| 6 | BE | -2.83 | 0 | 2.26 | [39] |
| ◆ | TFE | -1.07 | 910 | 0.87 | This |

*In the process of the present discussion, we realized numerical errors in the original paper ref. [38]. The present list values are duly corrected. The uncertainties in the values of a, b, and D are $a$ = -1.07 ± 0.05, $b$ = 910 ± 300 kJ/mol and $D$ = 0.87 ±0.09 for TFE, and $a$ = -1.16 ± 0.03, $b$ = 890 ± 300 kJ/mol and $D$ = 0.94± 0.07 for TBA.

**TOC graph**

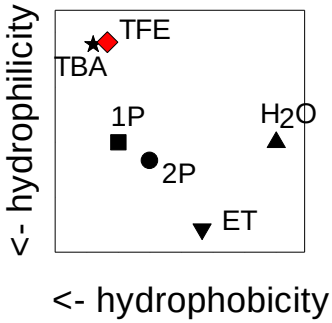


The net hydrophobicity of TFE is the same as that of TBA within the estimated uncertainty.